ELSEVIER

Chemical Engineering Journal 136 (2008) 227–235

Chemical Engineering Journal

www.elsevier.com/locate/cej

Concentration-dependent branched pore kinetic model for aqueous phase adsorption

Qipeng Jia, Aik Chong Lua *

School of Mechanical and Aerospace Engineering, Nanyang Technological University, 50 Nanyang Avenue, Singapore 639798, Republic of Singapore

Received 9 June 2006; received in revised form 29 March 2007; accepted 1 April 2007

Abstract

A model that takes into account of a concentration-dependent intra-particle effective surface diffusion coefficient in the branched pore kinetic model is presented. This model was applied to adsorption data obtained from the adsorption of phenol solution by activated carbons prepared from oil-palm shells. Parametric sensitivity analyses were carried out to study the effects of each parameter on the kinetic process. The simulations showed good agreement with experimental adsorption results. The introduction of a concentration-dependent effective surface diffusion coefficient provides a scheme to distinguish the intra-particle mass transfer mechanism for specific adsorption systems using kinetic experimental data. The concentration-dependent branched pore kinetic model is able to correlate together the adsorbent surface characteristics, the adsorbate properties and the adsorption kinetics.

Keywords: Aqueous phase adsorption; Branched pore kinetic model; Activated carbons; Phenol adsorption; Adsorption isotherms

1. Introduction

Adsorption process has been employed extensively in large scale for chemical and environmental separation engineering. Adsorption of proteins on solid surfaces and their interaction are major concerns in a number of fields such as biology, medicine, biotechnology and food processing, and play an important role from various points of view [1,2]. For its large specific surface area, activated carbon is a general adsorbent for the removal of many toxic compounds in environmental [3,4] and pharmaceutical applications [5]. Besides conducting adsorption tests to determine the effectiveness of any adsorbents, kinetic modelling is also needful to understand the physics of the adsorption process.

Kinetic models have successfully predicted numerous batch reactor adsorbate concentration profiles and provided significant insights on the way adsorbents function. In the absence of any external heat, the uptake rate in a particle exposed to a small change in concentration is determined by the rate of external mass transfer and intra-particle transport. Thus, the rate of adsorption in porous adsorbents is generally controlled by transport within the pore network. This intra-particle diffusion may occur by several different mechanisms depending on the pore size, the adsorbate concentration and other conditions. The internal diffusion for an activated carbon in an aqueous system can be described as surface diffusion [6], pore diffusion [7,8] or a combination of surface and pore diffusion [9,10] for mass transfer within the adsorbent. The diffusion coefficient may therefore be determined by matching the experimental uptake curve to the solution of the kinetic model [11].

The branched pore kinetic model (or the multi-pore model) [12,13] has been widely used to determine adsorption parameters and kinetics in liquid phase adsorption studies by activated carbons. The simulation results of Peel et al. [12] and Tien [13] showed that this model could be used to simulate the adsorption kinetics in a batch system for organic solution adsorption by activated carbons. In the model, the pore size distribution of the activated carbon is required as input to the mass balance equations. The pore structures consist of both rapidly and slowly diffusing regions. The model was developed to overcome problems arising from a single rate parameter analysis and was shown to describe the experimental data well. Recently, the applications of the branched pore kinetic model to aqueous phase activated carbon adsorption data have increased. Ko et al. [14] assessed

* Corresponding author. Tel.: +65 67905535; fax: +65 67924062.
E-mail address: maclua@ntu.edu.sg (A.C. Lua).

1385-8947/$ – see front matter © 2007 Elsevier B.V. All rights reserved.
doi:10.1016/j.cej.2007.04.005

Nomenclature

a_L	Langmuir isotherm equation constant ($l\,mg^{-1}$)
c	aqueous phase concentration ($mg\,l^{-1}$)
c_0	initial aqueous solution concentration ($mg\,l^{-1}$)
c_{eq}	equilibrium aqueous phase concentration ($mg\,l^{-1}$)
$C_{s,t}$	aqueous phase concentration at particle surface at time t ($mg\,l^{-1}$)
C_t	aqueous phase concentration at time t ($mg\,l^{-1}$)
D_{eff}	effective surface diffusion coefficient ($cm^2\,s^{-1}$)
$D_{eff,0}$	effective surface diffusion coefficient at zero loading ($cm^2\,s^{-1}$)
D_m	molecular diffusion coefficient in the bulk phase ($cm^2\,s^{-1}$)
E	binding energy ($kJ\,mol^{-1}$)
f	fraction of the total adsorptive capacity utilized in non-micropore region
FBiot	modified film Biot number (FBiot = $K_f c_0 R/\rho f D_{eff,0} q_0$)
ΔH_s	isosteric heat of adsorption ($kJ\,mol^{-1}$)
k	correlation constant in kinetic model
k_L	Langmuir isotherm equation constant ($l\,g^{-1}$)
K	Freundlich isotherm equation constant $(mg\,g^{-1})\,(l\,mg^{-1})^{n_F}$
K_b	branched micropore rate coefficient (s^{-1})
K_f	external aqueous phase mass transfer coefficient ($cm\,s^{-1}$)
n_F	Freundlich isotherm equation constant
N_{pt}	number of points on a fitted experimental curve
PBiot	modified particle Biot number (PBiot = $K_b R^2/f D_{eff,0}$)
q	adsorption capacity ($mg\,g^{-1}$)
q_0	solid phase concentration in equilibrium with c_0 ($mg\,g^{-1}$)
q_{av}	amount adsorbed on the adsorbent ($mg\,g^{-1}$)
q_b	solid phase concentration in micropore region ($mg\,g^{-1}$)
q_{eq}	equilibrium solid phase concentration ($mg\,g^{-1}$)
q_m	solid phase concentration in non-micropore region ($mg\,g^{-1}$)
q_{sat}	adsorbate concentration at surface saturation ($mg\,g^{-1}$)
r	radial distance from centre of particle (cm)
R	radius of particle (cm)
SFact	separation factor (SFact = $mq_0/V_f c_0$)
t	time (s)
V_f	solution volume (l)

Greek letters

ε	particle porosity
ρ	adsorbent particle density ($g\,cm^{-3}$)

the model for the adsorption of dyes onto activated carbon and bagasse pith in batch operations. Yang and Al-Duri [15] simulated the single component adsorption of three reactive dyes onto activated carbons in a batch stirred vessel with the model. In comparison to the many existing models, the branched pore model yielded more accurate results over a longer period of adsorption. It is reasonable to conclude that the multi-pore model is an intra-particle diffusion model proposed on the basis of the typical pore structures of activated carbons.

This paper presents a theoretical analysis of the adsorption kinetics of activated carbon in aqueous phenol solution. The adsorption of phenol onto a highly porous activated carbon prepared from a biomass was used to test the validity of the branched pore kinetic model. The concentration decays of adsorption process were fitted using the model and parameter sensitivity analyses were carried out to determine the influence of some parameters on the adsorption mechanism.

2. Model description

The branched pore kinetic model (BPKM) for aqueous phase activated carbon adsorption was proposed by Peel et al. [12]. The model depicted activated carbon adsorption as a dual mechanism rather than as a single mechanism process. In order to simulate the polydispersed or continuous pore size distributions of the activated carbon, the branched pore kinetic model divides the carbon pellets into rapidly and slowly diffusing regions. This division can also be reflected by the very different rates of diffusion in the two regions. It is difficult to deduce either the dimensions or relative proportions of the non-micropore and micropore regions. The regions are loosely termed as non-micropore and micropore regions. The fraction, f, is the amount of adsorption in the non-micropore region as compared to the total adsorptive capacity in the whole region. The initial rapid adsorptive uptake takes place in the non-micropore region. The remaining fraction, $1-f$, constitutes the adsorption in the micropore region. The model assumes that the distribution of both regions is radial and the diffusion between these two regions is expressed with a linear driving force between the local non-micropore and micropore concentrations. The assumption of the adsorption model for such a particle consists of three resistances in series: (1) diffusion of solute from solution, across the external liquid boundary layer onto the adsorbent external surfaces, then (2) diffusion into and adsorbing in the non-micropore region, and (3) diffusion into and adsorbing in the micropore region.

In adsorption simulation studies using the BPKM [12,14,15], the concentration-dependent surface diffusion coefficient is assumed as a constant and the values of the diffusion coefficients are determined by fitting the model to the experimental concentration decay curve. It is observed that although the simulation can cover a wide range of system conditions, the correlated surface diffusion coefficient in the non-micropore region increases with the initial aqueous solution concentration. Furthermore, the diffusivity is mathematically related to the amount of surface loading. So, an improvement is considered in this paper to introduce a concentration-dependent surface diffusion coefficient to improve the simulations and enable it possible to predict

the kinetics of the adsorption process with a single group of experimental data.

In this paper, the modes of mass transfer of the adsorbate molecules are outlined. The adsorbate molecules from the bulk fluid are transported through a stagnant boundary layer surrounding the adsorbent particle to the external surface of the particle by external diffusion. The mechanisms of intra-particle diffusion then proceed as follows. The adsorbate molecules on the particle surface migrate into the non-micropores by surface diffusion where the adsorbate molecules would be rapidly adsorbed onto the sorption sites. On the non-micropore surface, an adsorbed molecule may hop along the surface when it attains sufficient activation energy and when an adjacent adsorption site is available. This type of diffusion is referred to as surface diffusion. The adsorbed molecules on the non-micropore surfaces are mobile and migrate towards the micropores by surface diffusion and slowly adsorbed onto the micropore surfaces. The size of an adsorbate molecule is close to the size of the micropore and therefore surface diffusion becomes restricted; this would subsequently decrease the overall adsorption rate.

In the present model, an effective intra-particle surface diffusion mechanism is assumed to describe the intra-particle diffusion in the non-micropore region. In terms of an activation process, the effective surface diffusion coefficient of the intra-particle diffusion depends on the energy barrier for the diffusion of the adsorbate in the particle. The effective surface diffusion coefficient can be correlated with the solid phase concentration in a power expression [14]. In this paper, an exponential expression is adopted which correlates the concentration dependence of effective surface diffusion coefficient to the surface coverage of adsorbate molecules through the heat of the adsorption process [16]. The effective surface diffusion coefficient can be expressed as

$$D_{\text{eff}} = D_{\text{eff},0} \exp\left\{k\left(\frac{q}{q_{\text{sat}}}\right)\right\} \tag{1}$$

where D_{eff} is the effective surface diffusion coefficient (cm^2/s), $D_{\text{eff},0}$ the effective surface diffusion coefficient at zero surface coverage (cm^2/s), k the dimensionless constant, q the solid phase concentration (mg/g), and q_{sat} is the solid phase concentration at surface saturation (mg/g).

The orthogonal collocation method (OCM) was used to solve the partial differential equations in this concentration-dependent branched pore kinetic model (CDBPKM). With the OCM, the implicit scheme is not required for solving the complex non-linear PDEs. An optimizing method was used in fitting the adsorption rates in a batch system under a variety of operating conditions to determine various diffusion and physical parameters in the CDBPKM. The parameters are the external diffusion coefficient, K_{f}; the pre-exponential factor of the effective surface diffusion coefficient at the zero surface coverage, $D_{\text{eff},0}$; the fraction of non-micropore, f; the branched micropore rate coefficient, K_{b}; and the parameter, k, as defined in Eq. (1). The modelling studies were based on the adsorption of aqueous phenol solution onto activated carbons prepared from oil-palm shells in finite-batch systems.

3. Mathematical development

The governing equations of the proposed concentration-dependent branched pore kinetic model for predicting the adsorption process are given as follows.

The macroscopic mass conservation equation of the adsorbate in the aqueous phase is

$$V_{\text{f}}\frac{\text{d}C_t}{\text{d}t} = -m\frac{\text{d}q_{\text{av}}}{\text{d}t} \tag{2}$$

where m is the mass of the adsorbent, V_{f} the solution volume and C_t is the aqueous phase concentration at time t. The amount adsorbed in the solid phase, q_{av}, is

$$q_{\text{av}} = \frac{\int_V [fq_{\text{m}} + (1-f)q_{\text{b}}]\,\text{d}V}{V} \tag{3}$$

where f is the part of the total adsorptive capacity utilized in the non-micropore, q_{m} and q_{b} the solid phase concentrations in the non-micropore and micropore regions, respectively, and V is the volume of the adsorbent.

The non-micropore mass balance equation is

$$f\frac{\partial q_{\text{m}}}{\partial t} + (1-f)\frac{\partial q_{\text{b}}}{\partial t} = \frac{fD_{\text{eff},0}}{r^2}\frac{\partial}{\partial r}\left(r^2 \exp\left\{k\left(\frac{q_{\text{m}}}{q_{\text{msat}}}\right)\right\}\frac{\partial q_{\text{m}}}{\partial r}\right) \tag{4}$$

where $D_{\text{eff},0}$ is the effective surface diffusion coefficient at zero loading, r the radial distance from the centre of the adsorbent particle and q_{msat} is the adsorbate concentration in the non-micropore region at surface saturation.

The micropore mass balance equation is

$$(1-f)\frac{\partial q_{\text{b}}}{\partial t} = K_{\text{b}}(q_{\text{m}} - q_{\text{b}}) \tag{5}$$

where K_{b} is the branched micropore rate coefficient.

The coupling between the aqueous and solid phases achieved by equating the fluxes at the solid–aqueous interface is

$$K_{\text{f}}(C_t - C_{\text{s},t}) = fD_{\text{eff},0}\exp\left\{k\left(\frac{q_{\text{m}}}{q_{\text{msat}}}\right)\right\}\rho\left(\frac{\partial q_{\text{m}}}{\partial r}\right)_{r=R} \tag{6}$$

where K_{f} is the external aqueous phase mass transfer coefficient, $C_{\text{s},t}$ the aqueous phase concentration at the particle surface at time t, and ρ is the solid density of the adsorbent.

The local equilibrium at the interface between the aqueous and adsorbent solid phases is expressed in terms of the Langmuir isotherm as follows:

$$q_{\text{eq}} = \frac{k_{\text{L}}c_{\text{eq}}}{1 + a_{\text{L}}c_{\text{eq}}} \tag{7}$$

where c_{eq} and q_{eq} are the concentrations in the aqueous and solid phases, respectively, at equilibrium, and k_{L} and a_{L} are constants that correspond to monolayer coverage. The Langmuir isotherm equation is used instead of the Freundlich isotherm equation ($q_{\text{eq}} = Kc_{\text{eq}}^{1/n_{\text{F}}}$ where K and n_{F} are constants) and this will be discussed later on in the paper.

The initial and boundary conditions are as follows:

$$q_m(r,0)=0, \qquad q_b(r,0)=0, \qquad C_t(t=0)=c_0,$$
$$q_m(R,t)=q_s(t), \qquad \frac{\partial q_m}{\partial r}(0,t)=0 \tag{8}$$

The governing equations are non-dimensionlized using the following:

$$C=\frac{C_t}{c_0}, \qquad C_s=\frac{C_{s,t}}{c_0}, \qquad Q=\frac{q}{q_0},$$
$$\eta=\frac{r}{R}, \qquad \theta=\frac{D_{eff,0}t}{R^2} \tag{9}$$

A further independent variable, u, is introduced such that

$$u=\eta^2 \tag{10}$$

Substituting the dimensionless variables in Eqs. (9) and (10) into the differential-algebraic equation (DAE) system, i.e., Eqs. (4), (2), (5) and (6), respectively yield the following:

$$\frac{\partial Q_m}{\partial\theta}+\frac{1-f}{f}\frac{\partial Q_b}{\partial\theta}=4u\frac{\partial}{\partial u}\left[\exp\left\{k\left(\frac{Q_m}{Q_{m\,sat}}\right)\right\}\right]\frac{\partial Q_m}{\partial u}$$
$$+\exp\left\{k\left(\frac{Q_m}{Q_{m\,sat}}\right)\right\}\left[4u\frac{\partial^2 Q_m}{\partial u^2}+6\frac{\partial Q_m}{\partial u}\right] \tag{11}$$

$$\frac{\partial C}{\partial\theta}=-\mathrm{SFact}\left(f\int_V\frac{\partial Q_m}{\partial\theta}dV+(1-f)\int_V\frac{\partial Q_b}{\partial\theta}dV\right) \tag{12}$$

$$\frac{\partial Q_b}{\partial\theta}=\mathrm{PBiot}\frac{f}{1-f}(Q_m-Q_b) \tag{13}$$

$$\left(\frac{\partial Q_m}{\partial u}\right)_{u=1}=\left(\frac{\mathrm{FBiot}}{2}\right)\exp\left\{-k\left(\frac{Q_m}{Q_{msat}}\right)\right\}(C-C_s) \tag{14}$$

where the dimensionless parameters are given by the following:

$$\mathrm{FBiot}=\frac{K_f c_0 R}{\rho f D_{eff,0} q_0} \tag{15}$$

$$\mathrm{PBiot}=\frac{K_b R^2}{f D_{eff,0}} \tag{16}$$

$$\mathrm{SFact}=\frac{m q_0}{V_f c_0} \tag{17}$$

The Langmuir isotherm in Eq. (7) can be written as

$$Q_m|_{u=1}=\frac{C_s k_L c_0}{q_0+c_0 q_0 a_L C_s} \tag{18}$$

The initial and boundary conditions are now given by the following:

$$Q_m(\eta,0)=0, \qquad Q_b(\eta,0)=0, \qquad C(0)=1,$$
$$Q_m(1,t)=Q_s(t) \tag{19}$$

The method of orthogonal collocation was used to solve this DAE system. The method of orthogonal collocations on fixed elements was first introduced by Villadsen and Michelsen [17] and it was then applied to the adsorption processes in various studies [18–20]. This scheme requires that the normalized space coordinate r in the interval [0,1] be divided into N spatial domains with N interior collocation points plus the point at the boundary. After the discretization of the space coordinate in the N spatial domains, the approximation of the unknowns can be expressed by the polynomial functions. Substituting the discretized items into the equations, i.e., Eqs. (11)–(14), these items were calculated by integrating a system of ODEs and algebraic equations.

An optimizing subroutine based on the Levenberg–Marquardt non-linear regression was employed to search for the best combination of mass transfer coefficients. Data from the literature were used as the initial values for some of the dimensionless parameters.

4. Experimental

4.1. Material and analytical method

The activated carbons used in the adsorption tests were prepared from oil-palm shells. First, the raw shells were crushed and sieved to a size range of 2–2.8 mm. The shells were then carbonized under vacuum in a vertical stainless steel reactor at a heating rate of 10 K/min and heated to a final temperature of 673.15 K. The resulting chars were then transferred to another reactor and heated at the same rate as above to a final temperature of 1173.15 K under a nitrogen flow. At this final temperature, nitrogen flow was cut off and steam was introduced to activate the chars for 1 h. The activated carbons were characterized by a scanning electron microscope and an accelerated surface area and porosimetry system (ASAP 2010, Micromeritics) using N_2 adsorption at 77 K.

The phenol adsorbate used in the adsorption tests was obtained from Merck & Co., Inc., Germany. The adsorption capacity of the activated carbons was determined from the phenol solution concentration; this concentration was measured by a gas chromatograph–mass spectrometer (6890 N, GC-5973N MSD system, Agilent) using a HP-5MS column.

4.2. Adsorption equilibrium experiments

Phenol solution of different concentrations was prepared in the conical flasks. Each flask, containing 50 ml of the phenol solution, was immersed in a water bath at a pre-set temperature. After the adsorbate solution had stabilized, an accurate weighed amount of the activated carbon was added into the flask. The vibratory action of the bath was kept at 150 rpm until the solution had attained equilibrium. Two control flasks were set up. One flask, containing the phenol solution only, was to check for phenol volatilization and/or adsorption on the flask wall during the equilibration period. The other flask, containing deionized water and activated carbon, was to check the existence of organic contamination in the adsorbent and/or in the deionized water. After the phenol solution in the test flask had reached equilibrium, 1 ml of the supernatant was removed for analysis.

4.3. Kinetic experiments

The equilibrium adsorption isotherms and adsorption kinetics were determined by a batch method. The concentration of the phenol solution used was 180 mg/l and 50 ml of this solution in a conical flask was used for each kinetic test. With a known weight of activated carbon adsorbent added to the flask, it was then placed in a water bath at a pre-set temperature and agitated at a speed of 150 rpm. Samples of 1 ml were removed from the flask at regular time intervals and its concentration was measured. A plot of the adsorbate concentration versus time would depict the concentration decay characteristics of the phenol solution.

5. Results and discussion

5.1. Activated carbon characteristics

Fig. 1 shows the microstructure of the oil-palm-shell activated carbon used in the adsorption equilibrium and kinetic tests. The pores are generally homogeneous and distributed uniformly over the carbon surface. Fig. 2 shows the pore distribution of the activated carbon; it consists of a microporous and mesoporous

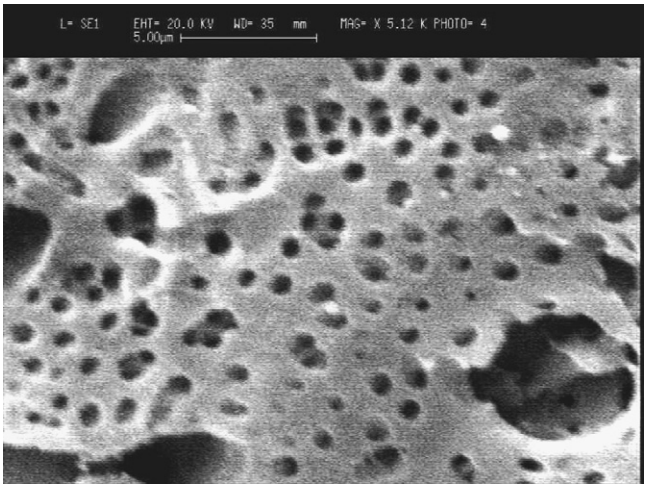

Fig. 1. Scanning electron micrograph of the activated carbon (5120×).

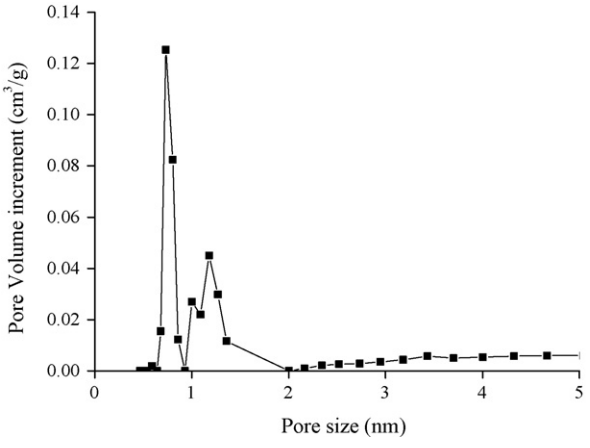

Fig. 2. Pore size distribution of the activated carbon.

Table 1
Physical characteristics of the activated carbon prepared from oil-palm shell

BET surface area ($m^2\ g^{-1}$)	1182.76
Pore volume ($cm^3\ g^{-1}$)	0.69
Non-micropore surface area ($m^2\ g^{-1}$)	354.33
Non-micropore volume ($cm^3\ g^{-1}$)	0.38
Average pore size (nm)	2.33

pore structure which is suitable for aqueous phase adsorption. Table 1 shows the physical characteristics of the activated carbon used in the adsorption studies.

5.2. Equilibrium adsorption isotherms

The equilibrium adsorption isotherm in Fig. 3 shows the adsorption capacity of phenol onto the activated carbon for various initial phenol concentrations. Using the experimental data, the adsorption isotherms based on the Langmuir and the empirical Freundlich equations were obtained based on the non-linear data fitting scheme in the least squares method. Comparisons of the Langmuir and Freundlich isotherms with the experimental data are given in Fig. 3 as well. The Langmuir isotherms fit the experimental data very well. Further, to quantify the validity of the two isotherms equations, the normalized and the non-normalized RMS (root mean square) residuals were computed. The non-normalized RMS residual weighs the actual error at all the points and is therefore more sensitive to errors at high equilibrium solution concentrations. The normalized RMS is based on the relative error and therefore weights all points equally. The formulae of the normalized RMS and the non-normalized RMS residuals are as follows:

$$\text{normalized RMS} = 100 \times \sqrt{\frac{1}{N_{pt}} \sum_{i=1}^{N_{pt}} \left(\frac{q_{ei,exp} - q_{ei,calc}}{q_{ei,exp}} \right)^2} \quad (20)$$

$$\text{non-normalized RMS} = \sqrt{\frac{1}{N_{pt}} \sum_{i=1}^{N_{pt}} (q_{ei,exp} - q_{ei,calc})^2} \quad (21)$$

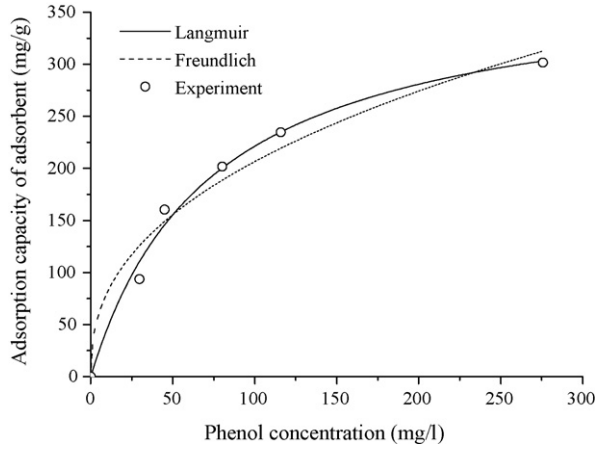

Fig. 3. Phenol adsorption isotherm at 30 °C: experimental vs. theoretical.

Table 2
Langmuir and Freundlich isotherm parameters and residual errors

Langmuir isotherm parameters	
k_L (l g^{-1})	5.22
a_L (l mg^{-1})	0.014
NRMS (%)	9.10
NNRMS	10.08
Freundlich isotherm parameters	
K (mg g^{-1}) (l mg^{-1})^{n_F}	31.41
n_F	0.41
NRMS (%)	16.36
NNRMS	18.44

where N_{pt} is the number of experimental points, and $q_{ei,exp}$ and $q_{ei,calc}$ are the experimental and calculated adsorption capacities, respectively. Table 2 lists the Langmuir and the Freundlich isotherm parameters and the residual errors. The results from the normalized and non-normalized RMS analyses again confirmed that the experimental data have better agreement with the Langmuir isotherm equation than the Freundlich isotherm equation.

5.3. Parametric estimation by the CDBPKM

The present model can be utilized to study the influence of individual parameter on the overall adsorption process. The various parameters in the model can be determined by fitting them to the experimental results. For the batch kinetic adsorption tests, identical operating conditions prevailed except for the different initial phenol concentrations used. Using the Langmuir isotherm equation, the experimental data were regressed using the CDBPKM in a non-linear least-square scheme and values of the fitted parameters are given in Table 3. The agreement between the experimental data and the present model is excellent as shown in Fig. 4, verifying the validity of the model. The average correlation coefficient of 0.98 as given in Table 3 further indicates the good agreement between the model and the experimental results. Comparing the mass transfer coefficients of K_f, $D_{eff,0}$ and K_b, it is clear that the rate controlling steps are the diffusion rates within the pore structures of the adsorbent particle. The relative importance of each of the five parameters (i.e., K_f, $D_{eff,0}$, K_b, f and k) can be assessed by the sensitivity analyses. For each parameter, the average value was obtained from the values given in Table 3 and used in the analyses. Varying one parameter at a time, the effect of each parameter on the adsorption kinetics using the present model can be demonstrated. For each particular parameter under study, three values were used: the average value, half and twice this average value. The remaining four parameters were held constant, based on their average value. The effects of the physical properties of the parameters on the aqueous phase concentration decay curve will be analyzed later. First, a discussion of the parameters follows next.

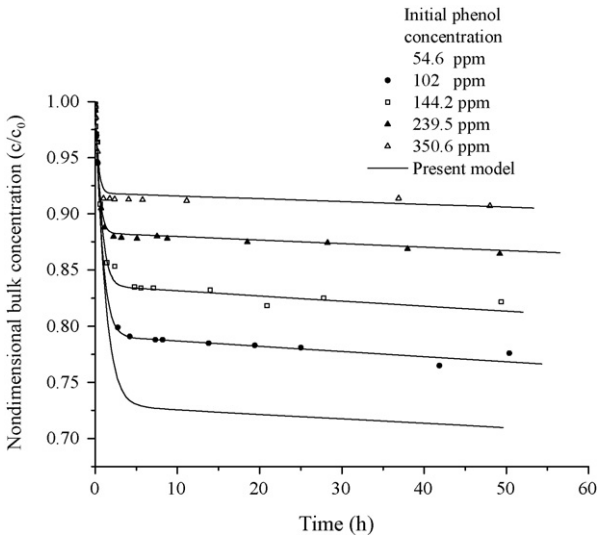

Fig. 4. Batch kinetic adsorption tests for different phenol concentrations.

5.3.1. The external (film) mass transfer coefficient K_f

The external mass transfer coefficient K_f is a function of the thickness of the boundary layer surrounding the adsorbent and the hydrodynamic flow field. For the adsorption tests in this present study, K_f should be fairly constant because of the constant agitation speed used in the water bath and the relatively narrow range of adsorbent sizes used. The small variation in the K_f values presented in Table 3 was probably due to the slight changes in the adsorbent mass used in the tests. The K_f value was evaluated from the initial bulk concentration data when the intraparticle diffusion resistance was negligible and subsequently adjusted during the optimization process.

5.3.2. The effective surface diffusion coefficient $D_{eff,0}$

The effective surface diffusion coefficient $D_{eff,0}$ in the adsorbent particle depends on the diffusion coefficient in the bulk phase and the detailed pore structure. The effective surface diffusion coefficient in the particle can be considered to be proportional to the diffusion coefficient in the bulk phase. So, the initial estimated effective surface diffusion coefficient can be obtained by the following expression:

$$D_{eff,0} = \varepsilon^2 D_m \quad (22)$$

Table 3
Various calculated parameters using the CDBPKM

c_0 (mg l^{-1})	Mass of adsorbent (mg)	N (rpm)	K_f (cm s^{-1})	$D_{eff,0}$ (cm^2 s^{-1})	K_b (s^{-1})	f	k	Correlation coefficient
350.6	13.08	150	1.38E−1	3.96E−7	2.42E−7	0.36	0.23	0.98
239.5	14.93	150	1.34E−1	3.54E−7	2.13E−7	0.36	0.23	0.98
144.2	14.09	150	1.29E−1	3.02E−7	2.50E−7	0.36	0.32	0.98
102	15.02	150	1.38E−1	3.46E−7	1.89E−7	0.36	0.25	0.99
54.6	15.06	150	1.41E−1	2.63E−7	1.11E−7	0.37	0.37	0.98

where ε is the porosity of the adsorbent particle and D_m is the molecular diffusion of the adsorbate. Molecular diffusion coefficients of organic molecules of low molecular weights in water are in the range of 10^{-6} to 1.5×10^{-5} cm^2 s^{-1} and it can be smaller with increasing molecular weight.

5.3.3. The parameter k

The parameter k is a quantitative measure of the binding energy to the differential heat of adsorption. It is proportional to ϕ where $\phi = E/(-\Delta H_s)$ [16]; E is the binding energy of the surface diffusion process and ΔH_s is the enthalpy change on adsorption or commonly referred to as the isosteric heat of adsorption. An increasing value of k indicates that an adsorbate molecule will be more readily adsorbed onto the pore surface by the surface diffusion process.

5.3.4. The micropore rate coefficient K_b

The micropore rate coefficient K_b is highly dependent on the pore radius within the micropore structure of the adsorbent. Decreasing pore radius in the micropore increases the energy barrier in the surface migration process, thereby greatly reducing its rate of diffusion. Also, the rate of micropore diffusion is a strong function of the solute diameter/pore diameter ratio. The initial value of K_b was assumed to be of the same magnitude of the effective surface diffusion coefficient, $D_{eff,0}$.

5.3.5. Fraction of total adsorptive capacity in non-micropores f

The fraction of total adsorption in non-micropore f depends on the properties of both the adsorbate and the adsorbent, even though it may seem to be a structural property. The fraction of the non-micropore surface area to the total pore surface area of the activated carbon is 0.3 as given in Table 1, which is smaller than the estimated value of f by the model. The difference suggests that some of the smaller micropores may not be accessible to the larger molecular size of phenol as compared to the molecular size of N_2 used in obtaining the adsorption isotherms for the determination of the pore surface area of the activated carbon. The initial value of f used was based on the fraction of non-micropore surface area to the BET surface area of the activated carbon.

5.4. Parameter sensitivity analysis

Parameter sensitivity analysis can provide an indication of the relative importance of each parameter defined in the present model. The five kinetic parameters for the phenol adsorption process have been used in the simulations to obtain the aqueous phase concentration decay curves. Fig. 5 shows that the aqueous phase concentration is a function of the external aqueous film mass transfer coefficient K_f and the duration of adsorption, if the other parameters are fixed. It shows that a lower K_f inevitably will result in a longer time to achieve a final equilibrium aqueous phase concentration. For values of $K_f = 0.68 \times 10^{-1}$, 1.36×10^{-1} and 2.72×10^{-1} cm s^{-1}, the times required to attain equilibrium concentration are about 5.5, 3.5 and 2 h, respectively. This shows that doubling K_f does not halve the equilibrium time. Fig. 6 shows that varying non-micropore surface diffusion coefficient, $D_{eff,0}$, has limited effect on the initial uptake period and thereafter there is small variability in the three concentration decay curves. This is expected because the adsorption in the non-micropore takes place first and once these sites are filled, the effect of $D_{eff,0}$ diminishes. Fig. 7 shows the effect of the micropore rate coefficient K_b on the aqueous bulk concentration decay curves. Varying K_b values only impact the later part of the uptake period as the micropores will be the last to be filled. Increasing K_b increases adsorption and therefore results in decreasing aqueous equilibrium concentration. The effect of the fraction of non-micropore, f, in Fig. 8 has the greatest impact on the aqueous bulk concentration amongst the five kinetic parameters, thus demonstrating that aqueous adsorption takes place substantially in the non-micropores. Increasing f reduces the aqueous bulk concentration as more non-micropores are available for adsorption. Varying k values have marginal effects on the aqueous bulk concentration decay curves as shown in Fig. 9. Increasing k increases the binding energy of the surface diffusion process and therefore increases sorption during the early uptake stage before the final equilibrium concentration sets in.

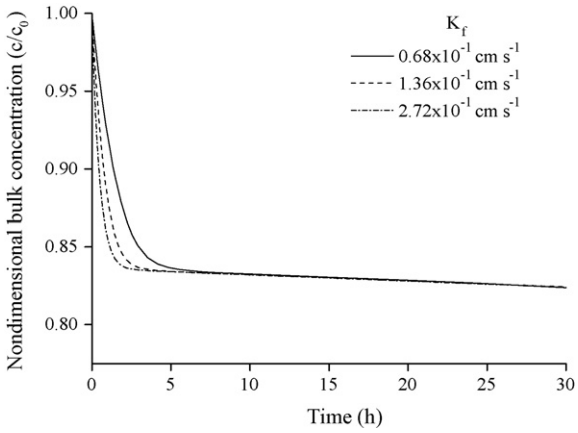

Fig. 5. Sensitivity analysis: K_f parameter ($D_{eff,0} = 3.32 \times 10^{-7}$ cm^2 s^{-1}, $K_b = 2.01 \times 10^{-7}$ s^{-1}, $f = 0.36$, $k = 0.28$).

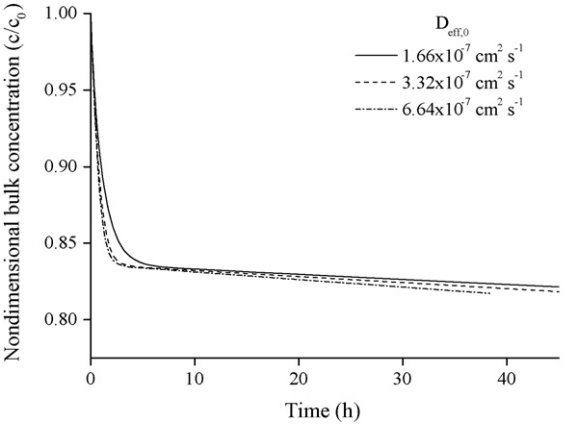

Fig. 6. Sensitivity analysis: $D_{eff,0}$ parameter ($K_f = 1.36 \times 10^{-1}$ cm s^{-1}, $K_b = 2.01 \times 10^{-7}$ s^{-1}, $f = 0.36$, $k = 0.28$).

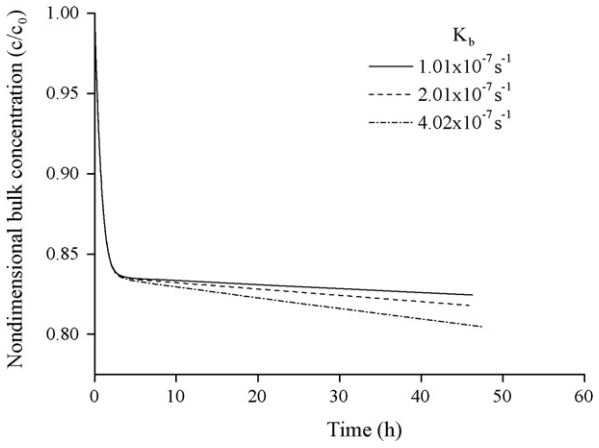

Fig. 7. Sensitivity analysis: K_b parameter ($K_f = 1.36 \times 10^{-1}$ cm s^{-1}, $D_{eff,0} = 3.32 \times 10^{-7}$ cm^2 s^{-1}, $f = 0.36$, $k = 0.28$).

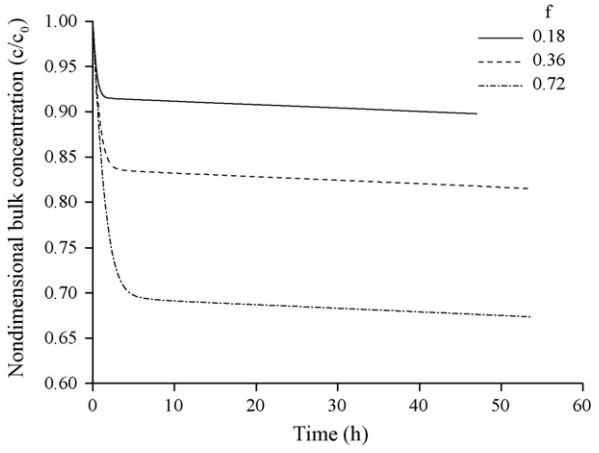

Fig. 8. Sensitivity analysis: f parameter ($K_f = 1.36 \times 10^{-1}$ cm s^{-1}, $D_{eff,0} = 3.32 \times 10^{-7}$ cm^2 s^{-1}, $K_b = 2.01 \times 10^{-7}$ s^{-1}, $k = 0.28$).

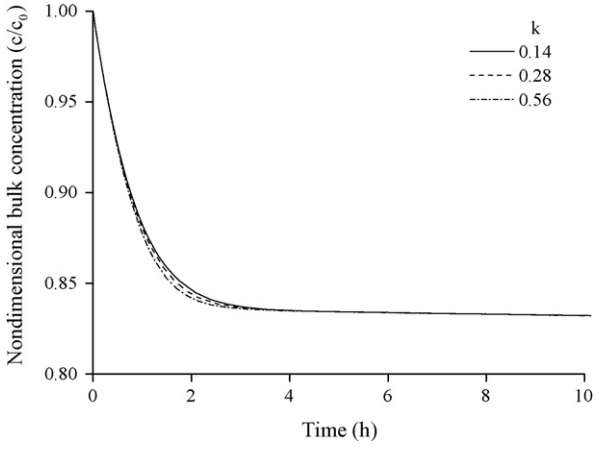

Fig. 9. Sensitivity analysis: k parameter ($K_f = 1.36 \times 10^{-1}$ cm s^{-1}, $D_{eff,0} = 3.32 \times 10^{-7}$ cm^2 s^{-1}, $K_b = 2.01 \times 10^{-7}$ s^{-1}, $f = 0.36$).

6. Conclusion

A mathematical model incorporating a concentration-dependent effective surface diffusion coefficient has been developed and applied to the aqueous phase adsorption of phenol onto activated carbon adsorbents with polydispersed pore structures. The validity of this model was tested by correlating the theoretical concentration decay curve with the experimental data and good agreement was obtained. Arising from this study, the pertinent points relating to this model are as follows:

1. The Langmuir equilibrium isotherm is more accurate than the Freundlich isotherm equations to describe the adsorption of aqueous phenol onto oil-palm-shell activated carbons.
2. The concentration-dependent branched pore kinetic model has been shown to be applicable and accurate for a wide range of experimental conditions prevailing in the adsorption system tested. The fraction of non-micropore structure has a fundamental and important effect on the adsorption process.
3. The validity of the model proves that the effective surface diffusion coefficient is a concentration-dependent parameter.

References

[1] K. Nakanishi, T. Sakiyama, et al., On the adsorption of proteins on solid surfaces, a common but very complicated phenomenon, J. Biosci. Bioeng. 91 (3) (2001) 233–244.
[2] W.D. Chen, X.Y. Dong, et al., Dependence of pore diffusivity of protein on adsorption density in anion-exchange adsorbent, Biochem. Eng. J. 14 (1) (2003) 45–50.
[3] A. Dabrowski, P. Podkoscielny, et al., Adsorption of phenolic compounds by activated carbon—a critical review, Chemosphere 58 (8) (2005) 1049–1070.
[4] N. Tancredi, N. Medero, et al., Phenol adsorption onto powdered and granular activated carbon, prepared from eucalyptus wood, J. Colloid Interf. Sci. 279 (2) (2004) 357–363.
[5] K.A.V. Kamp, D. Qiang, et al., Modified Langmuir-like model for modeling the adsorption from aqueous solutions by activated carbons, Langmuir 21 (1) (2005) 217–224.
[6] V.K.C. Lee, G. McKay, Comparison of solutions for the homogeneous surface diffusion model applied to adsorption systems, Chem. Eng. J. 98 (3) (2004) 255–264.
[7] K.K.H. Choy, J.F. Porter, et al., Film-pore diffusion models—analytical and numerical solutions, Chem. Eng. Sci. 59 (3) (2004) 501–512.
[8] C.W. Cheung, J.F. Porter, et al., Removal of Cu(II) and Zn(II) ions by sorption onto bone char using batch agitation, Langmuir 18 (3) (2002) 650–656.
[9] M. Polakovic, T. Gorner, et al., Kinetics of salicylic acid adsorption on activated carbon, Langmuir 21 (7) (2005) 2988–2996.
[10] A. Leitao, A. Rodrigues, The simulation of solid–liquid adsorption in activated carbon columns using estimates of intraparticle kinetic parameters obtained from continuous stirred tank reactor experiments, Chem. Eng. J. Biochem. Eng. J. 58 (3) (1995) 239–244.
[11] D.N. Jaguste, S.K. Bhatia, Combined surface and viscous flow of condensable vapor in porous media, Chem. Eng. Sci. 50 (2) (1995) 167–182.
[12] R.G. Peel, A. Benedek, et al., A branched pore kinetic model for activated carbon adsorption, AIChE J. 27 (1) (1981) 26–32.
[13] C. Tien, Adsorption Calculations and Modeling, Butterworth-Heinemann, Boston, 1994.
[14] D.C.K. Ko, D.H.K. Tsang, et al., Applications of multipore model for the mechanism identification during the adsorption of dye on activated carbon and bagasse pith, Langmuir 19 (3) (2003) 722–730.
[15] X.Y. Yang, B. Al-Duri, Application of branched pore diffusion model in the adsorption of reactive dyes on activated carbon, Chem. Eng. J. 83 (1) (2001) 15–23.
[16] E.R. Gilliland, R.F. Baddour, et al., Diffusion on surfaces. I. Effect of concentration on the diffusivity of physically adsorbed gases, Ind. Eng. Chem. Fundam. 13 (2) (1974) 95–100.

[17] J. Villadsen, M.L. Michelsen, Solution of Differential Equation Models by Polynomial Approximation, Prentice-Hall, Englewood Cliffs, NJ, 1978.

[18] G. McKay, Solution to the homogeneous surface diffusion model for batch adsorption systems using orthogonal collocation, Chem. Eng. J. 81 (1–3) (2001) 213–221.

[19] T.T. Lee, F.Y. Wang, et al., Dynamic simulation of bioreactor systems using orthogonal collocation on finite elements, Comput. Chem. Eng. 23 (9) (1999) 1247–1262.

[20] S. Arora, S.S. Dhaliwal, et al., Solution of two point boundary value problems using orthogonal collocation on finite elements, Appl. Math. Comput. 171 (1) (2005) 358–370.